



AlphaFill: enriching AlphaFold models with ligands and cofactors

Received: 10 December 2021

Accepted: 18 October 2022

Published online: 24 November 2022

Check for updates

Maarten L. Hekkelman ^{1,2}, Ida de Vries ^{1,2}, Robbie P. Joosten ^{1,3} & Anastassis Perrakis ^{1,3}

Artificial intelligence-based protein structure prediction approaches have had a transformative effect on biomolecular sciences. The predicted protein models in the AlphaFold protein structure database, however, all lack coordinates for small molecules, essential for molecular structure or function: hemoglobin lacks bound heme; zinc-finger motifs lack zinc ions essential for structural integrity and metalloproteases lack metal ions needed for catalysis. Ligands important for biological function are absent too; no ADP or ATP is bound to any of the ATPases or kinases. Here we present AlphaFill, an algorithm that uses sequence and structure similarity to ‘transplant’ such ‘missing’ small molecules and ions from experimentally determined structures to predicted protein models. The algorithm was successfully validated against experimental structures. A total of 12,029,789 transplants were performed on 995,411 AlphaFold models and are available together with associated validation metrics in the alphafill.eu databank, a resource to help scientists make new hypotheses and design targeted experiments.

Predicting the three-dimensional (3D) structure of a protein based on its amino-acid sequence alone has been a major scientific challenge for decades. Recently, artificial intelligence approaches, as implemented in the AlphaFold¹ and the RoseTTAFold² methods, have made protein structure prediction unprecedently reliable. Both approaches predict domain structures with impressive accuracy, but flexible parts of the protein (such as loops or intrinsically disordered regions) are understandably predicted with lower accuracy and confidence. Predictions for the proteomes of 48 different organisms, as well as all SWISS-PROT³ entries, have been publicly available in the AlphaFold protein structure database⁴—about a million predicted protein structures—at the time of this study, and more than 200 million followed in July 2022. These predicted models are already providing invaluable new biological insights regarding protein function.

The artificial intelligence prediction algorithms have not been trained to solve the protein folding problem from first principles. They have merely, yet impressively, learned the inherent rules of protein folding based on extensive training on experimentally

resolved structures. However, many proteins do not occur in nature without their cofactor: myoglobin or hemoglobin need a heme to fold; zinc-finger domains are not stable without a zinc ion and many proteins can only exist as homo- or hetero-multimers⁵. The multimer issue was addressed by the development of AlphaFoldMultimer⁶ and RoseTTAFold⁷, that can predict complex protein assemblies. However, predicted structural models exclusively account for the 20 canonical amino-acid residues, and do not predict the coordinates for small molecules, ligands and cofactors typically associated with a protein.

Here, we enrich the models in the AlphaFold database by ‘transplanting’ small molecules and ions that have been experimentally observed in homologous protein structures. The AlphaFill procedure we present has been validated against experimental structures and applied to all AlphaFold models to create a new resource, the AlphaFill databank, which is designed to help life scientist to easily generate new hypotheses for protein function and formulate relevant research questions.

¹Oncode Institute and Department of Biochemistry, The Netherlands Cancer Institute, Amsterdam, the Netherlands. ²These authors contributed equally: Maarten L. Hekkelman, Ida de Vries. ³These authors jointly supervised this work: Robbie P. Joosten, Anastassis Perrakis. e-mail: r.joosten@nki.nl; a.perrakis@nki.nl

Table 1 | Examples of frequently transplanted compounds in the AlphaFill databank for indicative levels of sequence identity: trans., transplants

Sequence identity		25%		30%		50%		70%	
Compound code and name	No. of entries	No. of transplants							
Nucleotides									
ADP Adenosine diphosphate	100,258	242,131	77,591	166,420	26,804	42,189	10,076	13,975	
AMP Adenosine monophosphate	59,639	102,608	44,548	68,972	12,811	18,334	3,951	4,881	
ATP Adenosine triphosphate	67,807	119,001	51,155	83,267	14,729	22,765	5,226	7,223	
GDP Guanosine diphosphate	30,839	77,253	23,810	51,240	10,986	16,702	4,831	6,353	
GTP Guanosine triphosphate	18,274	30,586	14,443	23,841	5,139	7,974	2,054	2,896	
UDP Uridine diphosphate	17,717	25,197	11,119	14,091	2,787	3,184	858	1,040	
Cofactors									
COA Coenzyme A	19,037	61,080	12,344	40,880	3,162	11,751	1,369	3,109	
FAD Flavin adenine dinucleotide	18,406	50,295	10,851	23,667	3,111	4,564	1,470	1,958	
FMN Flavin mononucleotide	11,892	26,072	7,732	15,929	2,611	4,054	1,225	1,719	
GSH Glutathione	9,764	20,884	7,535	14,186	2,113	3,021	851	1,122	
HEM Heme	18,675	45,968	11,586	28,849	6,000	13,737	4,242	7,850	
NAD Nicotinamide adenine dinucleotide	35,016	82,533	24,284	50,799	8,542	14,186	3,087	4,898	
NAI NADH	17,223	24,848	11,370	15,858	2,881	3,858	796	1,125	
NAP NAD phosphate/NADP	26,467	67,179	18,142	38,576	4,355	8,286	1,577	2,311	
NDP NADPH	21,598	42,241	14,291	26,603	3,660	7,383	1,535	2,937	
PLP Pyridoxal phosphate	13,462	158,684	10,119	94,516	5,016	12,904	2,131	4,978	
SAH S-Adenosyl-L-homocysteine	21,121	30,189	15,692	19,778	4,184	5,079	1,399	1,629	
SAM S-adenosylmethionine	21,072	32,467	16,239	23,465	4,449	7,361	1,890	2,948	
Miscellaneous									
CLA Chlorophyll A	3,505	443,127	3,217	425,290	1,502	171,022	1,375	157,851	
CLR Cholesterol	8,533	53,500	4,310	18,184	532	1,654	339	866	
Metal ions									
CA Calcium(²⁺) ion	202,360	759,181	145,813	473,734	40,010	117,321	15,910	47,819	
K Potassium(¹⁺) ion	117,813	270,758	86,633	189,961	23,999	51,361	7,239	13,707	
MG Magnesium(²⁺) ion	328,108	1,981,187	264,320	1,576,629	95,618	514,634	33,595	91,445	
NA Sodium(¹⁺) ion	272,353	1,067,005	204,482	734,824	57,076	176,645	19,793	53,329	
ZN Zinc(²⁺) ion	186,268	639,282	135,426	417,736	41,808	99,486	16,675	36,315	

Results

Transplanting compounds to AlphaFold models

First, we search for sequence homologs for each structure in the AlphaFold database in the PDB-REDO databank⁸. We consider structures with identity higher than 25% over an aligned sequence of at least 85 residues as hits. The most common ligands in the PDB, as well as cofactors and their analogs from the CoFactor database⁹ are kept as candidates for the ‘transplants’. Currently, we are transplanting 2,694 different compounds that represent over 95% of all ligand occurrences in the Protein Data Bank (PDB)¹⁰.

Next, the selection of structures with compounds of interest are structurally aligned¹¹ on the C α -atoms of the AlphaFold model, and the root-mean-square deviation (r.m.s.d.) is calculated (global r.m.s.d.). Starting from the closest homolog, all backbone atoms within 6 Å from the atoms of each compound that will be considered for ‘transplantation’ are selected and used for a local structural alignment to the AlphaFold model; the r.m.s.d. from this alignment is also calculated (local r.m.s.d.). Compounds are then transplanted into the AlphaFold model to make the AlphaFill model, unless the same compound has

already been placed within 3.5 Å of the centroid of the compound to be fitted (originating from a previously considered homolog). All AlphaFill models and metadata are stored in the AlphaFill databank.

Further details on the procedure are available in the Methods.

The AlphaFill databank

Applying the AlphaFill approach to the AlphaFold database available in February 2022 (995,411 models) resulted in 586,137 models that had at least one transplanted compound. A total of 12,029,789 compounds were transplanted into these models. A selection of frequently transplanted compounds is listed in Table 1, including their ‘transplantation’ frequency at four levels of sequence identity (25, 30, 50 and 70%), which we chose empirically. The numbers for all transplanted compounds at 25, 30, 40, 50, 60 and 70% are available from the AlphaFill website.

All AlphaFill models are available from <https://alphafill.eu> through a web-based user interface. To enable integration of AlphaFill data in other websites, a 3D-Beacons API (<https://github.com/3D-Beacons>) is implemented, which is already in use to show AlphaFill entries in the PDBe-Knowledge Base¹². In addition, the whole databank, including

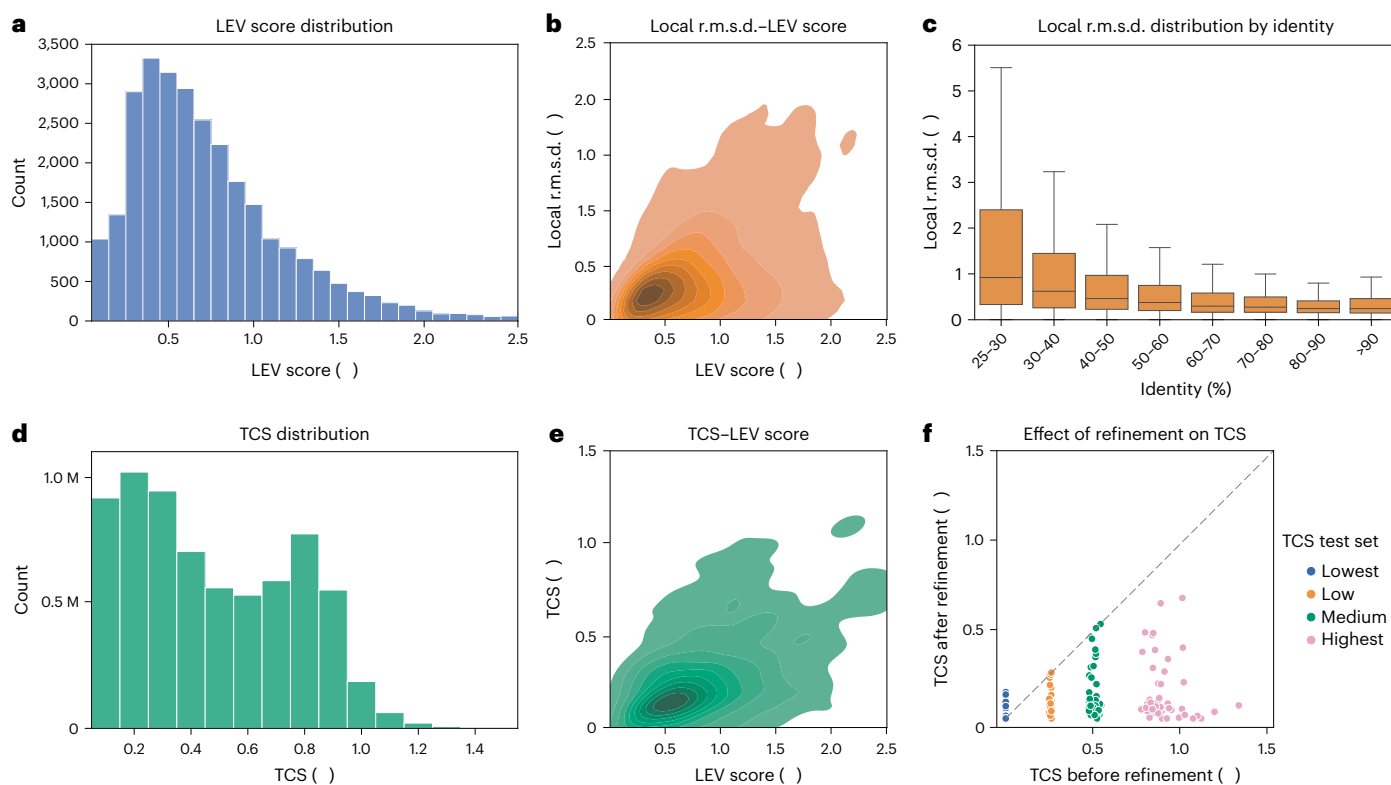


Fig. 1 | Validation of the AlphaFill algorithm. **a**, Distribution of the LEV score of all transplants obtained with 100% sequence identity (the validation set with $n = 28,619$ independent observations). 408 transplants (1%) with LEV score >2.5 are not shown for clarity. **b**, The local r.m.s.d. correlates with the LEV score in the validation set, Pearson correlation coefficient 0.51 ($n = 8,039$; mono-atomic transplants were not used (main text)). **c**, Distribution of the local r.m.s.d. of all transplants in the AlphaFill models as boxplots in 10% identity ranges. Boxes are based on 3,594,940; 3,866,810; 2,079,705; 1,005,953; 495,357; 369,307; 268,904 and 252,681 transplants, respectively, and extend from first to third quartile with the median as the middle line. Whiskers extend to 1.5 times the interquartile

range. For clarity, 332,771; 333,325; 181,126; 79,594; 42,273; 34,634; 29,368 and 24,263 outliers, respectively, are not shown. Maximum values are 107.4, 82.1, 40.6, 37.1, 61.5, 44.4, 35.6 and 35.5 Å. **d**, The distribution of the TCS for all transplants in the AlphaFill models ($n = 6,859,380$). Mono-atomic transplants (5,170,409 compounds) are left out (main text). **e**, The TCS correlates with the LEV score in the validation set ($n = 8,039$; mono-atomic transplants were used (main text)), Pearson correlation coefficient 0.51. **f**, Comparison of the TCS before and after energy minimization for four subsets of the validation set (each with $n = 50$), illustrating that TCS improves for low until highest TCS by refinement.

all relevant metadata (that is, the JSON format description of all transplants for each AlphaFill model, a JSON schema with a complete description of these files and the current CIF file that describes the compounds that are considered for transfer) can be downloaded through rsync, alphafill.eu.

Validation of the AlphaFill algorithm

To validate the AlphaFill algorithm, we compared the transplants created by AlphaFill to experimental structures with 100% sequence identity. We defined the local environment validation (LEV) score as the all-atom r.m.s.d. of any ligand atom and all proteins' atoms within 6.0 Å from the ligand, between the AlphaFill and experimental complexes. The distribution of the LEV score for all AlphaFill structures within this validation set (28,619 transplants) is presented in Fig. 1a. As the LEV score can be known only when a sequence-identical experimental structure is available, we then compared it to the local r.m.s.d., which we calculate for every transplant as defined above. The LEV score and the local r.m.s.d. correlate well (Fig. 1b). As the local r.m.s.d. can thus be used as a proxy for the quality of each transplant, we analyzed its distribution as a function of sequence identity between the donor and the acceptor model. As expected, local r.m.s.d. goes down with increasing sequence identity (Fig. 1c).

An orthogonal way to validate the quality of a transplant is to evaluate possible clashes between ligand and protein atoms. For this purpose, we defined the transplant clash score (TCS) as a function of

the van der Waals overlaps between a transplanted ligand and its binding site (see Methods for details). The distribution of the TCS for all multi-atomic transplants is shown in Fig. 1d. Single atom compounds are overrepresented in the dataset (5,170,409 compounds) and have relatively few clashes, and were thus excluded in evaluating the TCS to avoid biasing the analysis. The TCS correlates well with the LEV score (Fig. 1e). High TCS can suggest an incompatible binding site, suboptimal performance of the AlphaFill algorithm in transplanting the ligand or that the AlphaFold model has local inaccuracies. In the last two cases, clashes could be resolved by local refinement. We thus implemented a procedure using YASARA¹³ to energy minimize a complex. To test this procedure, we chose four sets of 50 complexes each: two sets were defined as the transplants with the lowest and the highest TCS, and two additional categories were chosen around 0.25 and 0.50 Å based on visual inspection of the distribution (Fig. 1d). We then evaluated the TCS before and after energy minimization (Fig. 1f). The TCS slightly increased for some structures in the set with the lowest starting TCS, but is reduced (or unchanged in a few cases) in structures in the other three sets. As the four sets were chosen from the validation set above, we then compared the LEV score before and after energy minimization (Supplementary Fig. 1a). For the lowest and low set, the LEV score is not strongly affected by de-clashing. For medium and highest TCS scores, in many cases the LEV score improves while for others it does not, suggesting that such transplants should be treated with caution.



P29373

Cellular retinoic acid-binding protein 2

Structure file	https://alphafill.eu/v1/aff/P29373-F1
Metadata	https://alphafill.eu/v1/aff/P29373-F1/json
Original AlphaFold model	https://alphafold.ebi.ac.uk/entry/P29373

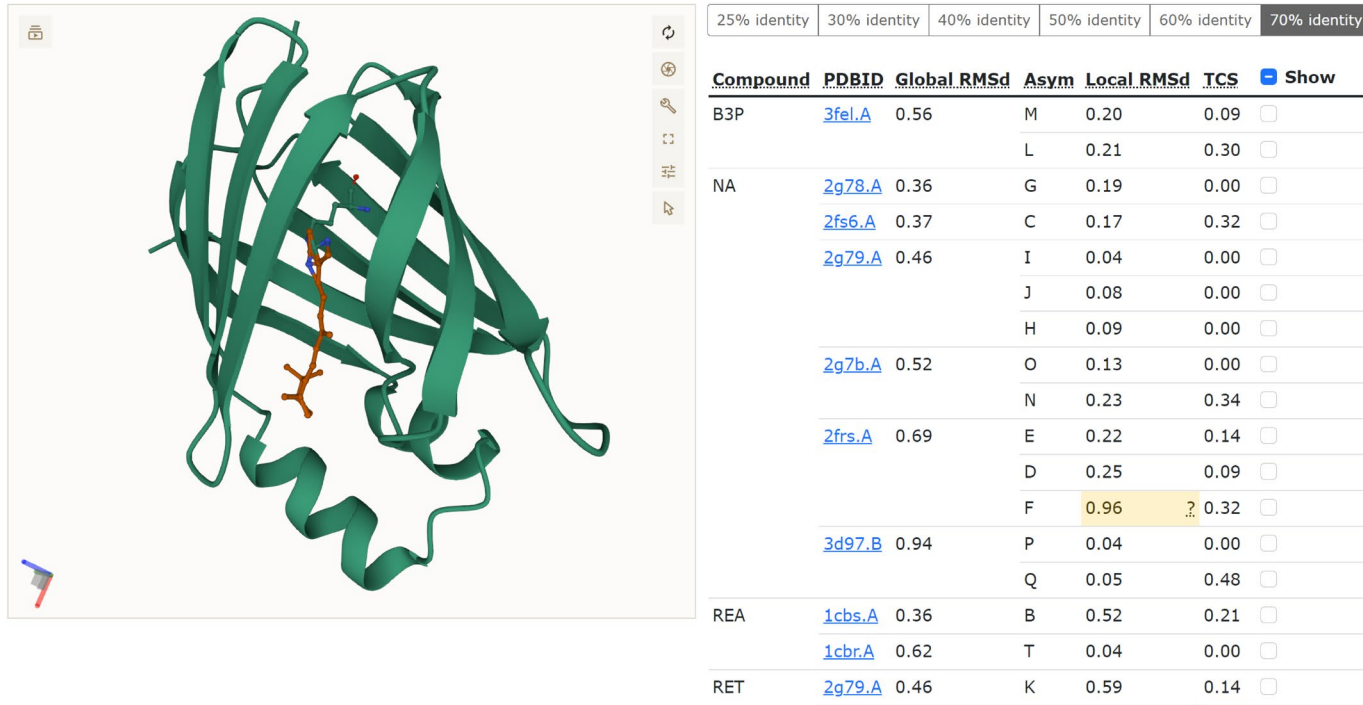


Fig. 2 | Screenshot of the AlphaFill entry page for cellular retinoic acid-binding protein 2 (AF-P29373). The Mol* viewer on the left can be controlled by the table of transplanted compounds on the right. Clicking a compound in the table brings up a zoom of the binding site. Compounds can be hidden or shown individually using the tick boxes. Transplants at 70% or more sequence identity are displayed. The identity cutoff can be changed using the selector above the

table. In this example, retinal (RET) inherited from PDB-REDO entry 4i9s (ref. ³⁶) is shown and flagged with a yellow box as medium confidence due to high TCS. All other transplanted compounds are hidden from view, providing the ‘optimise’ option for the selected transplant. After optimization (Supplementary Fig. 2) the TCS is reduced to 0.29 Å, which is considered high confidence. A sodium from PDB-REDO entry 2frs (ref. ³⁷) is flagged for its high local r.m.s.d.

Analysis of the quality of AlphaFill databank transplants

The validation was then used to derive quality indicators to annotate the transplants in the AlphaFill databank. As the local r.m.s.d. correlates well with the LEV score (Fig. 1b), we further analyzed its distribution as a function of sequence identity (Fig. 1c) to annotate the transplant. The local r.m.s.d. distribution stays fairly stable for structures with sequence identity of 70% or more (933,117 transplants). We use the values of the local r.m.s.d. exceeding the third quartile plus 1.5 times the interquartile range¹⁴ for all transplants with sequence identity of 70% or higher (0.92 Å) and for all transplants (3.10 Å) to annotate all AlphaFill transplants as ‘medium confidence’ and ‘low confidence’, respectively (Supplementary Fig. 1b). Using these cutoffs 65.3% of all transplants can be considered high confidence, 24.9% medium confidence and 9.9% low confidence. As the TCS also correlates well with the LEV score (Fig. 1e), we also use it to annotate transplants. Similar to the local r.m.s.d., we used the 1.5 interquartile range cutoff for 70% identity or higher (0.64 Å) and for all transplants (1.27 Å) (Supplementary Fig. 1c), to

assign high-confidence (81.3%), medium-confidence (18.6%) and low-confidence (0.05%) transplants based on TCS.

A web-based user interface for the AlphaFill databank

All AlphaFill entries are available for visual inspection through the AlphaFill website at <https://alphafill.eu>. On the front page, models can be retrieved using the AlphaFold identifier, which is equivalent to the UniProt primary accession code¹⁵. Individual entries can also be accessed directly using the same identifier, for example, <https://alphafill.eu/?id=P02144> for human myoglobin. The website makes the compound prevalence available (on the Compounds page), as well as numbers of occurrence regarding transplanted compounds for each ‘filled’ AlphaFold model (on the Structures page). The information on the Compounds and Structures pages can be filtered based on sequence identity at cutoffs of 25, 30, 40, 50, 60 and 70%.

On each entry page (Fig. 2) the selected AlphaFill model is displayed using the visualization software Mol*¹⁶, allowing users full flexibility for inspection. The ‘transplants’ are listed in a table together with

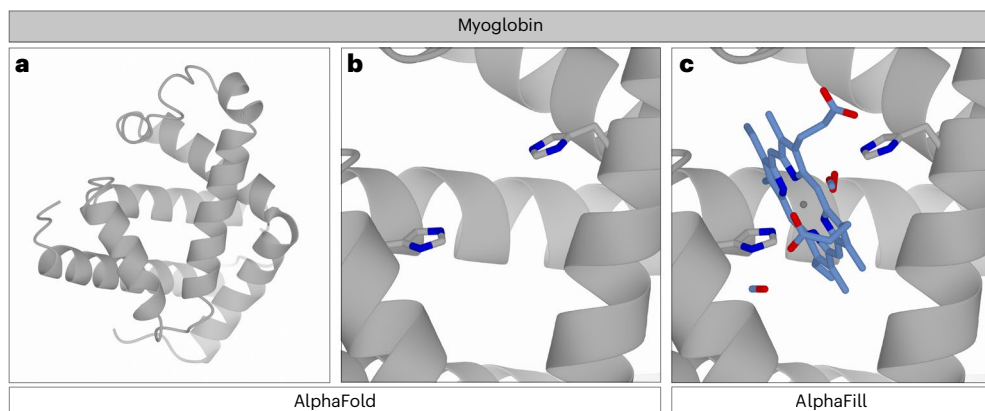


Fig. 3 | Human myoglobin structures in AlphaFold and AlphaFill. **a**, The ribbon diagram of the AlphaFold model of human myoglobin. **b**, The heme-shaped cavity in the AlphaFold model, wherein the histidine side chains (gray cylinders colored by atom type) are ready to facilitate the heme binding. **c**, The heme-

shaped cavity in the AlphaFill model, wherein the binding site is ‘filled’ with the transplanted heme group and the CO and O₂ ligands; ligands are shown in stick-mode colored by atom type (heme) with the heme iron as a gray sphere.

the parent PDB-REDO entry, the global r.m.s.d. between the AlphaFold model and for the hit within the PDB-REDO entry (as a measure of the similarity between the donor and the acceptor structure), the name of the compound (plus the original name if it was mapped), the local r.m.s.d. and the TCS (as quality indicators). Transplants are grouped by compound and sorted by r.m.s.d. (global at the hit level and local at the individual compound level). Clicking a row in the table changes the focus of the viewer to that compound. Compounds can also be toggled on and off to reduce clutter. Transplants are colored in the table by the local r.m.s.d.-based and the TCS-based confidence level (as defined above). Medium-confidence transplants that should be handled with care are marked in yellow; low-confidence transplants requiring caution are marked in red. Using the selector above the table, transplants can be shown at the levels of sequence identity described above. By default, the cutoff is set to the highest identity that displays hits in the table. In practice, this means that if the AlphaFold model can be mapped to an experimental structure with 93% sequence identity, by default only compounds transplanted from structures with more than 70% identity are shown; if only a 28% identical structure exists the default threshold will be set to 25%. When there is no transplant from an experimental structure with greater than 25% identity, the table is blank. A model with all the ligands and the metadata can also be downloaded. If a single transplant is selected in the table, the option to energy minimize (“optimise”) that particular transplant is made available to the user. Following optimization, the TCS score before and after refinement is shown, along with a ligand-focused view (Supplementary Fig. 2), and that particular optimized complex can be downloaded.

Examples

In the case of models that have identical structures in the PDB, the AlphaFill databank in part reproduces information already in the PDBe-Knowledge Base¹². However, AlphaFill also transplants compounds from homologous experimental structures that might have been determined in another species, and also to domains for which similar domains are available experimentally. Therefore, the databank offers additional functionality for the annotation of the models that can functionally assist users to make informed decisions about these structures. Here, we will discuss a few examples.

Myoglobin and heme

Human myoglobin is an α -helical protein with heme B as cofactor, binding molecular oxygen and several other small molecules. The AlphaFold model (AF-P02144) is nearly identical to experimentally determined structures, and shows a heme-shaped cavity (Fig. 3). In the AlphaFill

databank, many heme analogs (containing metals other than iron) are ‘mapped’ back to heme B (HEM, in PDB nomenclature) based on the data in CoFactor database. The heme analogs 6HE and 7HE that lack a carboxyl tail are not mapped back to heme B, but are instead transferred as is. Additional compounds that are transplanted to the AlphaFold myoglobin model include molecular oxygen and carbon monoxide. The latter is fitted on two locations: one close to the iron atom in heme and the other on the far side of the heme. The second carbon monoxide, located at an unexpected position, is inherited from PDB-REDO entry 1dwt (ref. ¹⁷), in which it was modeled at 30% occupancy. This occupancy is retained in the AlphaFill model to allow users to take this into account when evaluating the model. The AlphaFill model of myoglobin also contains numerous metal ions. The cobalt and nickel ions should be treated with care as they are inherited from engineered myoglobin dimers (PDB-REDO entries 7dgk and 7dgl, ref. ¹⁸) that do not have a normal myoglobin fold. This is clearly reflected by the global r.m.s.d. values being above 20 Å.

Zinc binding sites

The most common transition-metal ion present in macromolecular structures is zinc (Table 1). Typically, it is involved in catalysis or in maintaining structural integrity¹⁹. The so-called ‘structural zinc ions’ typically involve a tetrahedral binding site containing a combination of four coordinating cysteine and/or histidine residues²⁰. As we found before, such tetrahedrals are often distorted in the X-ray models available in the PDB, but the corresponding structures available through PDB-REDO contain improved binding sites²¹ and are better suited for usage in AlphaFill.

One of the proteins that contains both functional and structural zinc ions is the STAM-binding protein, a zinc metalloprotease that cleaves lysine-63-linked polyubiquitin chains (AF-O95630)²². Zinc ions have been transplanted to the AlphaFill model, both at the catalytic site and at the zinc-finger motif (Fig. 4a), originating from the PDB-REDO structure 3rzv (ref. ²³). The structural zinc ion is coordinated by three histidine residues and one cysteine. Although this tetrahedral zinc binding site looks proper, the atomic distances between the zinc atom and its ligands deviate from previously established target values²¹. This limitation is a consequence of AlphaFold predicting the structure outside the context of key structural elements, in this case the zinc ions. By adding the zinc atom, qualitative information is provided (the zinc atom should be in this binding site), but no quantitative information about the zinc binding site should be extracted from the AlphaFill model. Further refinement of the AlphaFill model with geometric restraints can be applied to make the binding site look more normal.

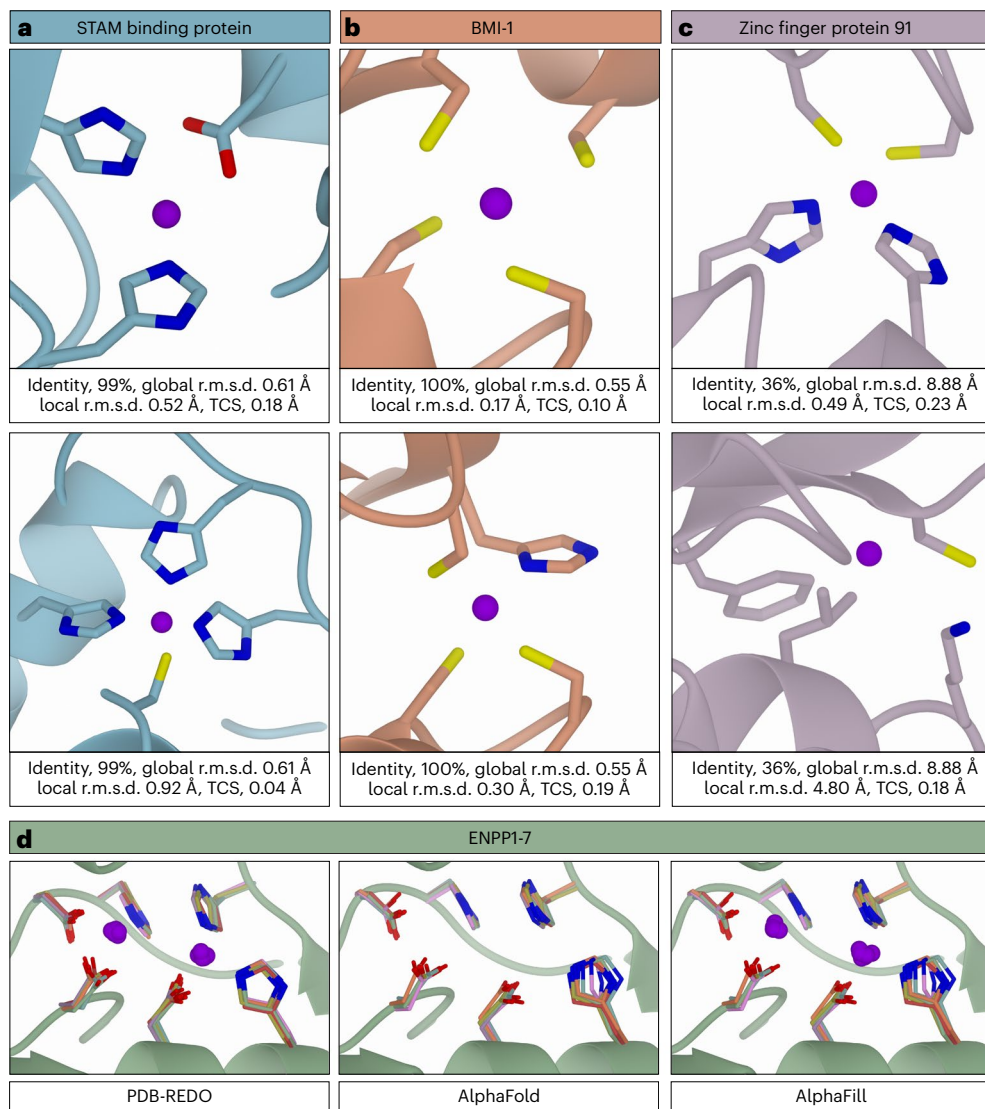


Fig. 4 | Examples of transplanted zinc ions (purple spheres). All proteins are presented as a ribbon diagram (each protein in a different color, for clarity); side chains coordinating the zinc ions are shown as cylinders colored by atom type for noncarbon atoms. **a**, A catalytic (top) and a structural (bottom) zinc ion in the STAM-binding protein. **b**, Two structural zinc ions in the human BMI-1. **c**, Zinc ion transferred into a structural zinc binding site in the zinc-finger protein 91 (top), wrongly placed zinc ion in the same protein (bottom). **d**, The bimetallic

zinc binding site in ENPP1-7 as found in PDB-REDO models (PDB identifiers for ENPP1-7: [6weu](#), ref. ³⁸; [5mhp](#), ref. ³⁹; [6c01](#), ref. ⁴⁰; [4lqy](#), ref. ⁴¹; [5veo](#), ref. ⁴²; [5egh](#), ref. ⁴³ and [5tcd](#), ref. ⁴⁴, respectively), compared to the same binding site as found in the human ENPP1-7 models from AlphaFold and as available in AlphaFill, containing the two zinc ions. For clarity, only the backbone of ENPP1 is shown as a green ribbon diagram; side chains are colored green, blue, red, pink, orange, purple and gold for ENPP1-7, respectively.

A similar situation is found for the two ‘transplanted’ zinc ions in the human BMI-1 protein ([AF-P35226](#)), which contains two zinc binding sites involved in structural integrity²³ (Fig. 4b). The binding sites are distorted in terms of coordination geometry with nonoptimal coordination distances and cysteine side chain conformations, but the fact that these are structural zinc binding sites is very clear. The two zinc atoms were transferred by AlphaFill from PDB-REDO entry [3rpg](#) (ref. ²³), completing the structural overview of BMI-1 with respect to structural integrity.

For ‘zinc-finger protein 91’, an E3 ubiquitin ligase upregulated in prostate cancer, colon cancer and pancreatic cancer²⁴, no experimental structures are available, but the human structure is predicted by AlphaFold ([AF-Q05481](#)). All transplanted zinc atoms have high global r.m.s.d. values (from 5.71 to 21.87 Å), but many have good local r.m.s.d. and TCS values. One such zinc atom is Zn AB originated in PDB-REDO entry [5wjq](#) (ref. ²⁵) (Fig. 4c). The global r.m.s.d. is high (8.88 Å), but the

local r.m.s.d. and TCS are good (0.49 and 0.23 Å, respectively); visual inspection shows that this zinc atom is biochemically sensible and has a normal binding site. Another zinc atom placed close to the same binding site (from PDB-REDO entry [6a57](#), ref. ²⁶) is marked unreliable based on the local r.m.s.d. value (4.80 Å); the positioning of this zinc ion is most likely incorrect (Fig. 4c).

In the ectonucleotide pyrophosphatase/phosphodiesterase (ENPP) family of proteins a bimetallic zinc site is important for catalysis^{27,28}. A structural alignment of the catalytic domain of PDB-REDO models of ENPP1-7 (Fig. 4d) shows that the zinc atoms and residues that coordinate them occupy highly similar positions in all family members. The AlphaFold predictions of the same proteins ([AF-P22413](#), [AF-Q13822](#), [AF-O14638](#), [AF-Q9Y6X5](#), [AF-Q9UJA9](#), [AF-Q6UWR7](#), [AF-Q6UWV6](#) for ENPP1-7, respectively) show more divergence, especially histidine R5 (Fig. 4d). AlphaFill picks up the similarity between the AlphaFold and the PDB-REDO models and transplants both zinc ions into the protein

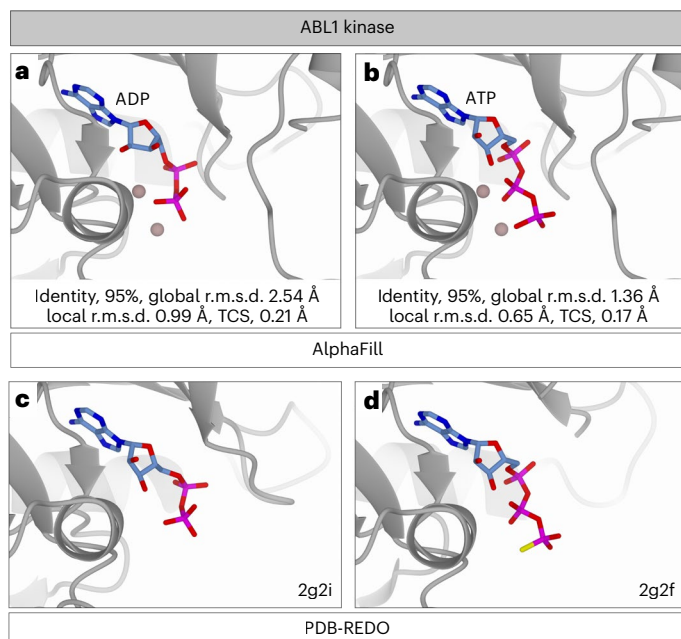


Fig. 5 | AlphaFill helps to understand the activation state of the Abl kinase AlphaFold model. **a**, AlphaFill model of the ABL1 kinase with ADP and magnesium ions shown. The state of the kinase is not known *a priori*. **b**, AlphaFill model of the ABL1 kinase with ATP (mapped from AGS) bound. **c**, ADP binding site of the human ABL1 kinase in PDB-REDO entry 2g2i (ref. ³⁰), which represents an active kinase state. **d**, ABL1 kinase bound with AGS in PDB-REDO entry 2g2f (ref. ³⁰), which represents an ‘intermediate’ kinase state. The kinase is presented as gray ribbon diagram for all panels, ligands are in blue cylinders colored by atom type for noncarbon atoms, and magnesium ions are shown as blush pink spheres.

models of ENPPs (Fig. 4d). Histidine R5 having different rotamers in the AlphaFold predictions, which based on the experimental structures should be a single rotamer, suggests that the bimetallic zinc site in the AlphaFill model(s) could benefit from additional refinement.

Kinases and ATP

Kinases are known to have multiple states between the active conformation that offers an environment conducive to the phosphotransfer reaction, and the inactive state that does not fulfill the chemical constraints required for catalytic activity²⁹. So far, AlphaFold provides only one conformation per protein. The state to which the AlphaFold models corresponds, is not known *a priori*. AlphaFill, however, transfers both ADP and ATP (or their analogs) to the AlphaFold model, provided that related experimental structures are available in the PDB-REDO database, regardless of the functional state of the kinase as characterized by the conformation of specific residues. For the human tyrosine-protein kinase ABL1 (AF-P00519) the AlphaFill model shows an ADP molecule and an ATP molecule (Fig. 5a,b) allowing different hypotheses for the functional state of this model. The global r.m.s.d. for the ADP source is 2.54 and for ATP 1.36 Å, while the local r.m.s.d. for ADP is 0.99 Å and for ATP 0.65 Å. This suggests that the structure is more representative of the ATP-bound state. The AlphaFill entry page informs the user that the ATP molecule was inherited from the ‘B’ chain of the experimental structure 2g2f with bound AGS (ATP-γ-S) (Fig. 5d), an ATP analog that promotes an ‘intermediate’ state in ABL1 (ref. ³⁰). Likewise, the ADP has been transplanted from PDB entry 2g2i (ref. ³⁰) (Fig. 5c), which represents an active state. Thus, the AlphaFill interface correctly highlights such differences, and allows a simple lookup of the underlying experimental models as well as associated literature to draw relevant conclusions.

Discussion

Analyzing the contacts of proteins to cofactors, ligands and ions, helps understand both the function and structural integrity of proteins. They can also be helpful for designing downstream experiments, either computational or in the wet laboratory. So far, the AlphaFold database does not include these compounds, but recognizes this need as for each predicted model links to experimental structures are provided through the PDBe-Knowledge Base¹². Here, we have presented the AlphaFill algorithm to create a resource that takes this further: we do not limit the ‘transplanting’ to the exact same protein, but we extend it to homologs of this model.

The current AlphaFill databank contains transplants of 2,694 different ligands, out of more than 30,000 in the PDB. These represent the most commonly occurring ligands as well as all the cofactors in CoFactor database, and cover about 95% of the cumulative occurrence of ligands in the PDB. We note, that the AlphaFill software is freely available (under the BSD license), which allows users to ‘submit’ any structural model for evaluation, and also the possibility to consider all >30,000 nonpolymer ligands in the PDB. An API to allow users to upload and ‘fill’ their own models or additional structures in the AlphaFold databank (added after June 2022) will be made available, also providing access to additional nonpolymer compounds from the PDB. We note, that currently AlphaFill does not handle polymer ligands, such as peptides, nucleic acids or sugars. It also does not handle posttranslational modifications and, in particular, glycosylation, which is a complicated matter that requires special attention³¹. Other posttranslational modifications such as phosphorylation, frequently induce conformational changes and are likewise not handled in AlphaFill.

An important decision parameter in the AlphaFill algorithm is the minimum sequence identity threshold to allow transfer of information from an experimental structure to an AlphaFold model. We superpose all experimental structures that showed more than 25% sequence identity with AlphaFold models, which also have an alignment length of at least 85 amino acids. This threshold is close to the minimal sequence identity requirement for structural homology³². We note that based on our experience with homology restraints⁸ and homology-based annotation of experimental structures³³ that a threshold closer to 70% is much more reliable for structural details such as local residue interactions; this threshold was also reflected in the validation analysis we present here (Fig. 1c). To allow users to explore possibilities, we have introduced a selector in the web interface that sets the display to the desired identity level on a per-structure basis.

Validation of AlphaFill models against experimental structures with 100% identity, has shown that the local r.m.s.d. and the TCS are good indicators for the reliability of a transplant. A clear color coding to draw the user’s attention to potentially erroneous transfers, indicating medium- and low-confidence transplants based on statistical distributions of these two criteria is used. We also offer the users to run on-the-fly energy minimization to optimize a particular complex of interest. We envisage that users will inspect choices, make selections and then optimize and download the optimized structures most relevant for their research.

The global r.m.s.d. is not a good indicators of transplant quality, but is useful to get a feeling of the similarity between the donor and acceptor structures: a structure with lower global r.m.s.d. but the same or similar identity, denotes a similar conformation. This is reflected in the kinase examples (Fig. 5). We also note that, for multi-domain proteins, the sequence alignment could span all structural domains, but the relative position of each domain might be different in the experimental structure and the model. In this case, the structural alignment may have inflated global r.m.s.d. values due to different relative domain positions. This was observed in the Zn transfer for zinc-finger protein 91 (Fig. 4c).

The AlphaFill structure models are not meant to be accurate or precise or complete representations of the full repertoire of ligands for a certain protein structure. They are meant as a tool for the nonexpert to help them explore complexes with common ligands. Structural biology or structural bioinformatics experts would find it trivial to select, superpose and ‘transplant’ a functional or structural cofactor or ion and take that information to be validated by molecular dynamics simulations and mutagenesis studies, or use it for discussing the structure of a model in light of new biochemical or biophysical insights.

It is good to keep in mind that the AlphaFill models are not very suitable for precise quantification of interactions between the transferred ligand(s) and the protein (for example, hydrogen bonds, π – π or cation– π interactions, van der Waals interactions, hydrophobic interactions, halogen bonds). Namely, this requires coordinate precision that is not provided by either the AlphaFold or the AlphaFill models (even after optimization). Hence, the models should be interpreted in a qualitative manner. Moreover, in some cases ligand interactions involve parts of the protein that are not modeled with high confidence by AlphaFold; while optimization might improve the local environment, we advise caution.

Besides using several optimized and robust defaults, the AlphaFill software is made to be flexible by design so that the used settings and cutoffs can easily be tailored to any user’s own purposes. Similarly, the list of transferrable compounds can readily be updated based on user requirements; we invite users to provide constructive feedback to allow to further develop these services.

AlphaFill by definition depends on high-quality structure homologs as the first and main criterion for transferring ligands. However, it is well established that certain structural domains can occur outside the context of extensive sequence similarity as it has been shown for example by DALI³⁴ and PDBeFold³⁵. Thus, AlphaFill could be complemented by structure-based transfer algorithms based on deep learning concepts similar to those used for the AlphaFold structure prediction revolution.

Online content

Any methods, additional references, Nature Portfolio reporting summaries, source data, extended data, supplementary information, acknowledgements, peer review information; details of author contributions and competing interests; and statements of data and code availability are available at <https://doi.org/10.1038/s41592-022-01685-y>.

References

1. Jumper, J. et al. Highly accurate protein structure prediction with AlphaFold. *Nature* **596**, 583–589 (2021).
2. Baek, M. et al. Accurate prediction of protein structures and interactions using a three-track neural network. *Science* **373**, 871–876 (2021).
3. Bairoch, A. & Apweiler, R. The SWISS-PROT protein sequence database and its supplement TrEMBL in 2000. *Nucleic Acids Res.* **28**, 45–48 (2000).
4. Tunyasuvunakool, K. et al. Highly accurate protein structure prediction for the human proteome. *Nature* **596**, 590–596 (2021).
5. Perrakis, A. & Sixma, T. K. AI revolutions in biology. *EMBO Rep.* **22**, e54046 (2021).
6. Evans, R. et al. Protein complex prediction with AlphaFold-Multimer. Preprint at <https://www.biorxiv.org/content/0.1101/2021.10.04.463034v1> (2021).
7. Humphreys, I. R. et al. Computed structures of core eukaryotic protein complexes. *Science* **10**, eabm4805 (2021).
8. van Beusekom, B. et al. Homology-based hydrogen bond information improves crystallographic structures in the PDB. *Protein Sci.* **27**, 798–808 (2018).
9. Fischer, J. D., Holliday, G. L. & Thornton, J. M. The CoFactor database: organic cofactors in enzyme catalysis. *Bioinformatics* **26**, 2496–2497 (2010).
10. Burley, S. K. et al. Protein Data Bank: the single global archive for 3D macromolecular structure data. *Nucleic Acids Res.* **47**, D520–D528 (2019).
11. Hanson, A. J. The quaternion-based spatial-coordinate and orientation-frame alignment problems. *Acta Cryst. A* **76**, 432–457 (2020).
12. PDBe-KB consortium. PDBe-KB: a community-driven resource for structural and functional annotations. *Nucleic Acids Res.* **48**, D344–D353 (2020).
13. Krieger, E. & Vriend, G. YASARA View—molecular graphics for all devices—from smartphones to workstations. *Bioinformatics* **30**, 2981–2982 (2014).
14. Tukey, J. W. *Exploratory Data Analysis* (Addison-Wesley, 1977).
15. The UniProt Consortium. UniProt: the universal protein knowledgebase in 2021. *Nucleic Acids Res.* **49**, D480–D489 (2021).
16. Sehnal, D. et al. Mol* Viewer: modern web app for 3D visualization and analysis of large biomolecular structures. *Nucleic Acids Res.* **49**, W431–W437 (2021).
17. Chu, K. et al. Structure of a ligand-binding intermediate in wild-type carbonmonoxy myoglobin. *Nature* **403**, 921–923 (2000).
18. Nagao, S., Idomoto, A., Shibata, N., Higuchi, Y. & Hirota, S. Rational design of metal-binding sites in domain-swapped myoglobin dimers. *J. Inorg. Biochem.* **217**, 111374 (2021).
19. Alberts, I. L., Nadassy, K. & Wodak, S. J. Analysis of zinc binding sites in protein crystal structures. *Protein Sci.* **7**, 1700–1716 (1998).
20. Torrance, J. W., MacArthur, M. W. & Thornton, J. M. Evolution of binding sites for zinc and calcium ions playing structural roles. *Proteins* **71**, 813–830 (2008).
21. Touw, W. G., van Beusekom, B., Evers, J. M. G., Vriend, G. & Joosten, R. P. Validation and correction of Zn–CysxHis γ complexes. *Acta Cryst. D* **72**, 1110–1118 (2016).
22. Davies, C. W., Paul, L. N., Kim, M.-I. & Das, C. Structural and thermodynamic comparison of the catalytic domain of AMSH and AMSH-LP: nearly identical fold but different stability. *J. Mol. Biol.* **413**, 416–429 (2011).
23. Bentley, M. L. et al. Recognition of UbcH5c and the nucleosome by the Bmi1/Ring1b ubiquitin ligase complex. *EMBO J.* **30**, 3285–3297 (2011).
24. Tang, N. et al. Zinc finger protein 91 accelerates tumour progression by activating β -catenin signalling in pancreatic cancer. *Cell Prolif.* **54**, e13031 (2021).
25. Patel, A. et al. DNA conformation induces adaptable binding by tandem zinc finger proteins. *Cell* **173**, 221–233.e12 (2018).
26. Tian, Z. et al. Crystal structures of REF6 and its complex with DNA reveal diverse recognition mechanisms. *Cell Discov.* **6**, 17 (2020).
27. Stefan, C., Jansen, S. & Bollen, M. NPP-type ectophosphodiesterases: unity in diversity. *Trends Biochem. Sci.* **30**, 542–550 (2005).
28. Borza, R., Salgado-Polo, F., Moolenaar, W. H. & Perrakis, A. Structure and function of the ecto-nucleotide pyrophosphatase/phosphodiesterase (ENPP) family: tidying up diversity. *J. Biol. Chem.* **298**, 101526 (2022).
29. Modi, V. & Dunbrack, R. L. Defining a new nomenclature for the structures of active and inactive kinases. *Proc. Natl Acad. Sci. USA* **116**, 6818–6827 (2019).
30. Levinson, N. M. et al. A Src-like inactive conformation in the Abl tyrosine kinase domain. *PLoS Biol.* **4**, e144 (2006).

31. Bagdonas, H., Fogarty, C. A., Fadda, E. & Agirre, J. The case for post-predictional modifications in the AlphaFold Protein Structure Database. *Nat. Struct. Mol. Biol.* **28**, 869–870 (2021).
32. Sander, C. & Schneider, R. Database of homology-derived protein structures and the structural meaning of sequence alignment. *Proteins* **9**, 56–68 (1991).
33. van Beusekom, B. et al. LAHMA: structure analysis through local annotation of homology-matched amino acids. *Acta Cryst. D* **77**, 28–40 (2021).
34. Holm, L. in *Structural Bioinformatics: Methods and Protocols* (ed. Gáspári, Z.) 29–42 (Springer, 2020).
35. Krissinel, E. & Henrick, K. Secondary-structure matching (SSM), a new tool for fast protein structure alignment in three dimensions. *Acta Cryst. D* **60**, 2256–2268 (2004).
36. Berbasova, T. et al. Rational design of a colorimetric pH sensor from a soluble retinoic acid chaperone. *J. Am. Chem. Soc.* **135**, 16111–16119 (2013).
37. Vaezeslami, S., Mathes, E., Vasileiou, C., Borhan, B. & Geiger, J. H. The structure of apo-wild-type cellular retinoic acid binding protein II at 1.4 Å and its relationship to ligand binding and nuclear translocation. *J. Mol. Biol.* **363**, 687–701 (2006).
38. Dennis, M. L. et al. Crystal structures of human ENPP1 in apo and bound forms. *Acta Cryst. D* **76**, 889–898 (2020).
39. Desroy, N. et al. Discovery of 2-[[2-ethyl-6-[4-[2-(3-hydroxyazetidin-1-yl)-2-oxoethyl]piperazin-1-yl]-8-methylimidazo[1,2-a]pyridin-3-yl]methylamino]-4-(4-fluorophenyl)thiazole-5-carbonitrile(glpg1690), a first-in-class autotaxin inhibitor undergoing clinical evaluation for the treatment of idiopathic pulmonary fibrosis. *J. Med. Chem.* **60**, 3580–3590 (2017).
40. Gorelik, A., Randriamihaja, A., Illes, K. & Nagar, B. Structural basis for nucleotide recognition by the ectoenzyme CD203c. *FEBS J.* **285**, 2481–2494 (2018).
41. Albright, R. A. et al. Molecular basis of purinergic signal metabolism by ectonucleotide pyrophosphatase/phosphodiesterases 4 and 1 and implications in stroke. *J. Biol. Chem.* **289**, 3294–3306 (2014).
42. Gorelik, A., Randriamihaja, A., Illes, K. & Nagar, B. A key tyrosine substitution restricts nucleotide hydrolysis by the ectoenzyme NPP5. *FEBS J.* **284**, 3718–3726 (2017).
43. Morita, J. et al. Structure and biological function of ENPP6, a choline-specific glycerophosphodiester-phosphodiesterase. *Sci. Rep.* **6**, 20995 (2016).
44. Gorelik, A., Liu, F., Illes, K. & Nagar, B. Crystal structure of the human alkaline sphingomyelinase provides insights into substrate recognition. *J. Biol. Chem.* **292**, 7087–7094 (2017).

Publisher's note Springer Nature remains neutral with regard to jurisdictional claims in published maps and institutional affiliations.

Open Access This article is licensed under a Creative Commons Attribution 4.0 International License, which permits use, sharing, adaptation, distribution and reproduction in any medium or format, as long as you give appropriate credit to the original author(s) and the source, provide a link to the Creative Commons license, and indicate if changes were made. The images or other third party material in this article are included in the article's Creative Commons license, unless indicated otherwise in a credit line to the material. If material is not included in the article's Creative Commons license and your intended use is not permitted by statutory regulation or exceeds the permitted use, you will need to obtain permission directly from the copyright holder. To view a copy of this license, visit <http://creativecommons.org/licenses/by/4.0/>.

© The Author(s) 2022

Methods

Detailed overview of the procedure

The AlphaFill procedure for filling up missing information to AlphaFold models goes through the following steps.

- (1) The amino-acid sequence of each AlphaFold model is BLASTed⁴⁵ against the sequence file of the LAHMA webserver³³, which contains all sequences present in the PDB-REDO databank. The alignments, that is individual high-scoring segment pairs (HSPs) are sorted by *E* value to capture both the sequence similarity and the length of the alignment as they are combined factors in conferring structural homology. A maximum of 250 hits, as is the default for BLAST, is returned.
- (2) The structure models corresponding to these hits are retrieved from the PDB-REDO databank and checked for compounds of interest for the AlphaFill algorithm (vide infra).
- (3) The hits with compounds of interest are filtered to ensure that only sufficiently close homologs are used. Currently, we use a sequence identity cutoff of 25% over an aligned HSP of at least 85 residues. For such an alignment length, identities as low as 25% still confer overall structural homology³².
- (4) This selection of hits is structurally aligned¹¹ on the α -atoms of the residues that match in the BLAST alignment. The r.m.s.d. of this global alignment is stored in the AlphaFill metadata. Note that a single PDB-REDO model chain can have several HSPs. These are aligned individually.
- (5) Starting from the hit with the smallest BLAST *E* value, each compound of interest in the hit list is scanned for its local surroundings. All backbone atoms within 6 Å are then used for a local structural alignment to the AlphaFold model. The r.m.s.d. of this local alignment is also stored in the AlphaFill metadata.
- (6) Compounds are then integrated into the AlphaFold model to make its AlphaFill counterpart, unless the same compound has already been placed within 3.5 Å of the centroid of the compound to be fitted (originating from a previously considered homolog) or no protein atoms are present within 4.0 Å from the atoms of the compound to be fitted. If compounds have multiple conformations, all of these are included in the AlphaFill model. Descriptions of covalent bonds or metal binding captured in so-called struct_conn records are also added to the AlphaFill model.
- (7) For each transplant a TCS is calculated using equation (1) and stored in the metadata. The TCS is the r.m.s. van der Waals overlap over all atomic distances between the transplant atoms and the protein that are shorter than 4 Å.

$$TCS = \sqrt{\frac{\text{vd Waals overlap}_i^2 + \text{vd Waals overlap}_j^2 + \text{vd Waals overlap}_k^2 + \dots}{\text{Number of distances considered}}} \quad (1)$$

- (8) The AlphaFill model with all transplanted compounds is finally stored as mmCIF coordinate file together with a JSON-formatted metadata file describing the provenance of each transplanted compound.

The running time per model depends strongly on the number of BLAST hits and compounds to be transferred. The mean running time is 2 minutes per model on a single CPU thread.

Input data: protein structure models

All AlphaFold models¹ (available 1 February 2021) were downloaded from the AlphaFold Protein Structure Database's FTP archive. A local copy of the PDB-REDO databank⁸ was used to provide ligands for transfer.

To find all relevant PDB-REDO entries for a specific AlphaFold model through sequence-based retrieval with BLAST, a

PDB-REDO-specific sequence database (as of 1 February 2021) was used. This database is created automatically as part of the weekly LAHMA and PDB-REDO databank updates.

Input data: selection of chemical compounds

We decided to only consider compounds that likely represent common biological states and are likely suited for further study. Thus, a collection of common biologically relevant cofactors, ligands and metal ions was created.

The selection of biological relevant ligands to be added to the AlphaFold models was performed based on the number of their occurrences in the PDB. All ligands covering about 95% of the cumulative occurrence of all ligands in the PDB were in the initial AlphaFill compound list that was complemented with all cofactors and their analogs present in the organic CoFactor database⁹ that were not within the 95% cumulative occurrence. To map cofactor analogs and adducts to their canonical cofactors where possible, analogs were mapped to their representative cofactor by atom renaming (and atom deletion); for example, adenosine-5'-(beta,gamma-methylene)triphosphate (methylene substituted ATP) is translated to ATP, as ATP is the compound involved in biological processes. Cofactor adducts such as CNC (vitamin B12 in complex with cyanide) are trimmed down to their parent (for example, vitamin B12 in the CNC case) by atom deletion. Cofactor analogs that have atoms missing with respect to their parent are kept as is. The required changes were found by visual inspection of the compounds via the Ligand-Expo website⁴⁶ and the PDB web sites. Common crystallization agents (for example, poly-ethyleneglycol and chloride), some metals with unclear physiological importance (for example, cadmium ions), posttranslational modifications (modified amino acids) and other polymers (peptides, nucleic acids and carbohydrates) were purposely excluded. All information was stored in a CIF-formatted data file that can easily be extended.

The current collection of compounds to be transplanted consists of 2,694 entries. It is stored separate from the AlphaFill program to allow easy extension in future incarnations of the AlphaFill databank and is freely available.

The AlphaFill software

A new program, AlphaFill, was created for the purpose of this study. AlphaFill reads an AlphaFold model together with the compound list and the PDB-REDO-specific sequence database and structures, and returns a structure model consisting of the coordinates of the AlphaFold model plus all transferred compounds. See above for the compound transfer procedure. The AlphaFill program is based on the libzeep^{47,48}, libcif++ (ref. ⁴⁹) (a general purpose C++ library for dealing with mmCIF data structures), libpdb-redo (a core library for PDB-REDO software) and clipper⁵⁰ libraries, and contains its own BLAST implementation. The source codes of AlphaFill, libcif++ and libpdb-redo are available from <https://github.com/PDB-REDO>.

Creation of the AlphaFill databank

The AlphaFill databank was created by running AlphaFill over all AlphaFold models. The computational workload is parallel that allows orchestration of the calculations by using the software make⁵¹, as we have done previously⁵², with the AlphaFold coordinate files as sources and the AlphaFill coordinate files as targets. The calculation took 15 days on a server with a total of 90 CPU threads.

The AlphaFill web interface

The web site was created as a web application using the libzeep library that offers an HTTP server, HTML templating and many other components for web server construction in C++. Handling of mmCIF files is done using libcif++. The data for the Models, Structures and Compounds pages are stored in a PostgreSQL⁵³ database. The model is presented on the page using Mol¹⁶ as an interactive web component.

Validation of the AlphaFill algorithm

To validate the AlphaFill algorithm, all transplanted compounds that were obtained from a donor PDB-REDO model with 100% sequence identity were selected as validation set (28,619 transplants). For each compound in this set, we calculated the all-atom r.m.s.d. with respect to the donor model for the transplant binding site that we called the LEV score. The transplant binding site consists of all nonhydrogen atoms of the transplant and all nonhydrogen protein atoms within 6.0 Å of the transplant atoms.

The LEV score was correlated to the local r.m.s.d. and to the TCS, which are both calculated in the AlphaFill algorithm for each transplant. The Pearson correlation coefficient was calculated using DataFrame. corr() in pandas v.1.2.4.

Model refinement

The AlphaFill web interface allows the refinement of individual transplants in the context of the protein. When a single transplant is selected, a user can activate its refinement. A new structure file containing only the protein and the selected transplant is created and passed to the refinement engine that runs on the server backend. The refinement procedure is based on the 'Energy minimization' experiment in YASARA¹³ that consists of a steepest descent minimization followed by a short simulated annealing in the updated YASARA NOVA⁵⁴ force field. All default settings are used and force-field parameters for the transplant are generated on-the-fly by YASARA. After the energy minimization, the TCS of the transplant is recalculated. The original and new TCS values are displayed together with a Mol* viewer of the refined model. The refined model can also be downloaded.

Validation of the refinement procedure

The refinement engine provides the option to energy minimize a specific transplant in complex with the protein on demand. To validate the refinement results, the TCS and LEV score before and after refinement were obtained and analyzed for four subsets of compounds in the validation set: (1) the 50 lowest TCS, (2) the 50 transplants with TCS closest to 0.25 Å, (3) the 50 transplants with TCS closest to 0.50 Å and (4) the 50 transplants with the highest TCS.

Model and data analysis

The AlphaFill models were analyzed visually using Coot⁵⁵, the AlphaFill website and CCP4mg (ref. ⁵⁶). Plots were made using Seaborn⁵⁷, molecular graphics figures were made with CCP4mg. Data analyses for validation were performed using Python v.3.7.9 with the numpy v.1.20.3 and pandas v.1.2.4 packages.

Reporting summary

Further information on research design is available in the Nature Portfolio Reporting Summary linked to this article.

Data availability

All input data used in this study are freely available from PDB-REDO (<https://pdb-redo.eu>), AlphaFold (<https://alphafold.ebi.ac.uk/>) and CoFactor (<http://www.ebi.ac.uk/thornton-srv/databases/CoFactor/>). All data discussed in this paper are publicly available from <https://alphafill.eu>. An individual AlphaFill entry (entryid) can be downloaded via the graphical user interface. In addition, structure files in mmCIF format are available for every entry at: [https://alphafill.eu/v1/aff/\\${entryid}.json](https://alphafill.eu/v1/aff/${entryid}.json). JSON files with the metadata for the transplants are available at: [https://alphafill.eu/v1/aff/\\${entryid}/json](https://alphafill.eu/v1/aff/${entryid}/json). The JSON schema providing details on the metadata is at <https://alphafill.eu/alphafill.json.schema>. The complete AlphaFill databank can be freely downloaded by the command: rsync -av rsync://rsync.alphafill.eu/alphafill {destination folder}/.

Code availability

The AlphaFill code used for this study is available through Zenodo at <https://zenodo.org/record/6706668#.Y2EXV3bP2Uk>. Current and future versions are open source with a BSD-2-clause license and available from <https://github.com/PDB-REDO/alphafill>.

References

45. Altschul, S. F., Gish, W., Miller, W., Myers, E. W. & Lipman, D. J. Basic local alignment search tool. *J. Mol. Biol.* **215**, 403–410 (1990).
46. Feng, Z. et al. Ligand Depot: a data warehouse for ligands bound to macromolecules. *Bioinformatics* **20**, 2153–2155 (2004).
47. Hekkelman, M. L. & Vriend, G. MRS: a fast and compact retrieval system for biological data. *Nucleic Acids Res.* **33**, W766–W769 (2005).
48. Hekkelman, M. L. mhekkel/libzeep: maintenance release. Zenodo <https://doi.org/10.5281/zenodo.5733933> (2021).
49. Westbrook, J. D. et al. PDB/mmCIF ecosystem: foundational semantic tools for structural biology. *J. Mol. Biol.* **434**, 167599 (2022).
50. Cowtan, KevinD. The Clipper C++ libraries for X-ray crystallography. *IUCr Computing Commission Newsletter* **2**, 4–9 (2003).
51. Feldman, S. I. Make—a program for maintaining computer programs. *J. Softw. Pract. Exp.* **9**, 255–265 (1979).
52. Joosten, R. P. et al. A series of PDB related databases for everyday needs. *Nucleic Acids Res.* **39**, D411–D419 (2011).
53. Stonebraker, M. & Rowe, L. A. The design of POSTGRES. *SIGMOD Rec.* **15**, 340–355 (1986).
54. Krieger, E. et al. Improving physical realism, stereochemistry, and side-chain accuracy in homology modeling: four approaches that performed well in CASP8. *Proteins* **77**, 114–122 (2009).
55. Emsley, P., Lohkamp, B., Scott, W. G. & Cowtan, K. Features and development of Coot. *Acta. Crystallogr. D. Biol. Crystallogr.* **66**, 486–501 (2010).
56. McNicholas, S., Potterton, E., Wilson, K. S. & Noble, M. E. M. Presenting your structures: the CCP4mg molecular-graphics software. *Acta. Cryst. D.* **67**, 386–394 (2011).
57. Waskom, M. L. seaborn: statistical data visualization. *J. Open Source Softw.* **6**, 3021 (2021).

Acknowledgements

We thank the Research High Performance Computing facility of the Netherlands Cancer Institute for providing and maintaining computation resources and S. McNicholas for support with CCP4mg. This work has been supported by iNEXT-Discovery, project number 871037 to A.P., funded by the Horizon 2020 program of the European Commission and by an institutional grant of the Dutch Cancer Society and of the Dutch Ministry of Health, Welfare and Sport. The funders had no role in study design, data collection and analysis, decision to publish, or preparation of the manuscript. We thank all colleagues at B8 for useful discussions and reading this manuscript, in particular, J. Bak, A. Murachelli, R. Xie, T. Brummelkamp and T. Sixma.

Author contributions

M.L.H. developed the AlphaFill software and web interface. I.d.V. analyzed chemical compounds for integration, worked on validation, data FAIRification and prepared the example cases and related figures. A.P. and R.P.J. conceived and supervised the project. All authors contributed to writing the manuscript, the experimental and algorithmic design and the analysis of the results.

Competing interests

The authors declare no competing interests.

Additional information

Supplementary information The online version contains supplementary material available at <https://doi.org/10.1038/s41592-022-01685-y>.

Correspondence and requests for materials should be addressed to Robbie P. Joosten or Anastassis Perrakis.

Peer review information *Nature Methods* thanks the anonymous reviewers for their contribution to the peer review of this work. Arunima, Singh was the primary editor on this article and managed its editorial process and peer review in collaboration with the rest of the *Nature Methods* team.

Reprints and permissions information is available at www.nature.com/reprints.

Reporting Summary

Nature Research wishes to improve the reproducibility of the work that we publish. This form provides structure for consistency and transparency in reporting. For further information on Nature Research policies, see our [Editorial Policies](#) and the [Editorial Policy Checklist](#).

Statistics

For all statistical analyses, confirm that the following items are present in the figure legend, table legend, main text, or Methods section.

n/a Confirmed

- The exact sample size (n) for each experimental group/condition, given as a discrete number and unit of measurement
- A statement on whether measurements were taken from distinct samples or whether the same sample was measured repeatedly
- The statistical test(s) used AND whether they are one- or two-sided
Only common tests should be described solely by name; describe more complex techniques in the Methods section.
- A description of all covariates tested
- A description of any assumptions or corrections, such as tests of normality and adjustment for multiple comparisons
- A full description of the statistical parameters including central tendency (e.g. means) or other basic estimates (e.g. regression coefficient) AND variation (e.g. standard deviation) or associated estimates of uncertainty (e.g. confidence intervals)
- For null hypothesis testing, the test statistic (e.g. F , t , r) with confidence intervals, effect sizes, degrees of freedom and P value noted
Give P values as exact values whenever suitable.
- For Bayesian analysis, information on the choice of priors and Markov chain Monte Carlo settings
- For hierarchical and complex designs, identification of the appropriate level for tests and full reporting of outcomes
- Estimates of effect sizes (e.g. Cohen's d , Pearson's r), indicating how they were calculated

Our web collection on [statistics for biologists](#) contains articles on many of the points above.

Software and code

Policy information about [availability of computer code](#)

Data collection	No specific data collection software was used. The AlphaFill code used for this study is available through Zenodo with DOI: 10.5281/zenodo.6706668. Current and future versions are open source with a BSD-2-clause license and available from https://github.com/PDB-REDO/alphafill .
Data analysis	Data analyses for validation were performed using Python3.7.9 with the numpy version 1.20.3 and pandas version 1.2.4 packages. Visual examination of models was performed with Coot versions 0.8.9.2 to 0.9.8.3.

For manuscripts utilizing custom algorithms or software that are central to the research but not yet described in published literature, software must be made available to editors and reviewers. We strongly encourage code deposition in a community repository (e.g. GitHub). See the Nature Research [guidelines for submitting code & software](#) for further information.

Data

Policy information about [availability of data](#)

All manuscripts must include a [data availability statement](#). This statement should provide the following information, where applicable:

- Accession codes, unique identifiers, or web links for publicly available datasets
- A list of figures that have associated raw data
- A description of any restrictions on data availability

All input data used in this study are freely available from PDB-REDO (<https://pdb-redo.eu>), AlphaFold (<https://alphafold.ebi.ac.uk/>), and CoFactor (<http://www.ebi.ac.uk/thornton-srv/databases/CoFactor/>).

All data created and discussed in this paper are publicly available from <https://alphafill.eu>. An individual AlphaFill entry (entryid) can be downloaded via the graphical user interface. In addition, structure files in mmCIF format are available for every entry at: "[https://alphafill.eu/v1/aff/\\${entryid}](https://alphafill.eu/v1/aff/${entryid})". JSON files with the meta-data for the transplants are available at: "[https://alphafill.eu/v1/aff/\\${entryid}/json](https://alphafill.eu/v1/aff/${entryid}/json)". The JSON-schema providing details on the metadata is at "[https://alphafill.eu/v1/aff/\\${entryid}/json](https://alphafill.eu/v1/aff/${entryid}/json)".

alphafill.eu/alphafill.json.schema". The complete AlphaFill databank can be freely downloaded by the command: "rsync -av rsync://rsync.alphafill.eu/alphafill {destination folder}".

The following license applies:

"Data files contained in the AlphaFill databank (rsync://rsync.alphafill.eu; https://alphafill.eu) are fully and freely available for both non-commercial and commercial use. Users of the data should attribute both AlphaFill and AlphaFold. By using the materials available in the AlphaFill, the user agrees to abide by the conditions described below:

* The archival data files in the AlphaFill archive are made freely available to all users. Data files within the archive may be redistributed in original form without restriction. Redistribution of modified data files is allowed only if the parent data file is attributed.

* Where applicable, the usage policy of the parent AlphaFold archive entries applies.

* The data in the AlphaFill databank are provided on an "as is" basis. Neither AlphaFill nor its parent or comprising institutions can be held liable to any party for direct, indirect, special, incidental, or consequential damages, including lost profits, arising from the use of AlphaFill materials.

* Resources on alphafill.eu are provided without warranty of any kind, either expressed or implied. This includes but is not limited to merchantability or fitness for a particular purpose. The institutions managing this site make no representation that these resources will not infringe any patent or other proprietary right.

Field-specific reporting

Please select the one below that is the best fit for your research. If you are not sure, read the appropriate sections before making your selection.

Life sciences Behavioural & social sciences Ecological, evolutionary & environmental sciences

For a reference copy of the document with all sections, see nature.com/documents/nr-reporting-summary-flat.pdf

Life sciences study design

All studies must disclose on these points even when the disclosure is negative.

Sample size	The sample consisted of all AlphaFold entries (February 2022), n = 995411
Data exclusions	No data were excluded
Replication	The study was computational and non-stochastic which made replication unnecessary. That is, any repeat calculation with the same input will return exactly the same results.
Randomization	Rather than performing calculations on random subsets of the AlphaFold Databank, the entire data set was considered. Therefore randomisation was not applicable as there is no sampling.
Blinding	The study was purely computational and contained no aspects where the use of blinding has any effect on the outcome of the performed calculations.

Reporting for specific materials, systems and methods

We require information from authors about some types of materials, experimental systems and methods used in many studies. Here, indicate whether each material, system or method listed is relevant to your study. If you are not sure if a list item applies to your research, read the appropriate section before selecting a response.

Materials & experimental systems

n/a	Involved in the study
<input checked="" type="checkbox"/>	<input type="checkbox"/> Antibodies
<input checked="" type="checkbox"/>	<input type="checkbox"/> Eukaryotic cell lines
<input checked="" type="checkbox"/>	<input type="checkbox"/> Palaeontology and archaeology
<input checked="" type="checkbox"/>	<input type="checkbox"/> Animals and other organisms
<input checked="" type="checkbox"/>	<input type="checkbox"/> Human research participants
<input checked="" type="checkbox"/>	<input type="checkbox"/> Clinical data
<input checked="" type="checkbox"/>	<input type="checkbox"/> Dual use research of concern

Methods

n/a	Involved in the study
<input checked="" type="checkbox"/>	<input type="checkbox"/> ChIP-seq
<input checked="" type="checkbox"/>	<input type="checkbox"/> Flow cytometry
<input checked="" type="checkbox"/>	<input type="checkbox"/> MRI-based neuroimaging